Evaluation of Russian Roulette and Particle Splitting Monte Carlo Methods for Space Radiation Transport

Rajarshi Pal Chowdhury, Luke A. Stegeman, Amir A. Bahadori

Kansas State University
Department of Mechanical and Nuclear Engineering
Ward Hall, 1200 N. 17th St, Manhattan, KS 66506, USA
rajarshipc@ksu.edu, lukesteg@ksu.edu, bahadori@ksu.edu

INTRODUCTION

A major obstacle for space missions outside of low-Earth orbit is the presence of high-energy heavy charged particles attributed to solar particle events (SPE) and galactic cosmic rays (GCR). SPEs contain mainly protons often accelerated as result of coronal mass ejections and solar flares [1]. These events can last hours or days, and can be intense enough to cause acute effects in humans. GCRs, on the other hand, mostly contain of protons and other heavy charged particles with atomic mass ranging from lithium to nickel, with kinetic energies ranging from MeV to ZeV [2]. GCRs in general contain 89% protons, 10% alphas and 1% heavier ions [3]. Always present and slowly varying, GCRs are primarily responsible for the long-term effects of space radiation, such as cancer [4].

In recent years, investment in long-term deep space missions, such as proposed missions to the Moon and Mars, has increased significantly [5]. Although the field of modern spacecraft shielding has expanded to include active methods of radiation shielding, passive shielding is still relevant for deep space missions. To minimize risk of space radiation-induced health effects, understanding optimum radiation shielding is crucial.

For the past several decades, deterministic transport methods have been favored for this task. Specifically, NASA uses HZETRN to evaluate radiation risk for current and proposed space missions [6-7]. Monte Carlo (MC) simulations are generally regarded as more accurate than current deterministic methods due to their more realistic representation of the three-dimensional (3D) nature of radiation interactions with complex geometries and consideration of all possible secondary particles. Significant advances have been made in the ability of HZETRN to address 3D radiation transport effects [8], but MC methods are still used for validation and verification [9]. Despite these advantages, MC simulations, such as those implemented in the Particle and Heavy Ion Transport code System (PHITS) [10], take a substantial amount of time to complete, even with access to modern high-performance computing systems. This excessive computation time makes MC methods unattractive for rapid prototyping of space radiation shielding systems.

In the present work, the Russian roulette/particle splitting variance reduction method [11] is explored as an alternative to the mostly-analog MC approaches usually used for space radiation transport. This method improves convergence by splitting particles that move toward the region of interest, reducing the weight of each to prevent bias in the tally. Particles that move away from the region of interest are killed with some probability; if the particle survives, its weight is increased accordingly.

Variance reduction via Russian roulette and particle splitting has been applied to many MC problems over the past several decades. However, no systematic study investigating the optimum number of importance regions for space radiation transport exists in literature. The purpose of the present study is to determine the number of equal-thickness importance regions providing the most efficient SPE MC simulation for materials and shielding thicknesses commonly encountered in space radiation protection problems.

DESCRIPTION OF THE ACTUAL WORK

Materials and Geometry

Various shielding configurations consisting of aluminum (Al) and high-density polyethylene (HDPE) were considered in this work. Shield thicknesses were varied from 5 g cm^{-2} to 100 g cm^{-2}, a reasonable range for realistic space radiation shielding geometries. The simulation geometry described by Slaba et al [12] has been replicated to account for backscatter provided by shielding past the region of interest, where the specified shielding thickness is placed both in front of and behind a thin layer of water. The water thickness was chosen to be 0.3 mm, and was divided into three regions of equal width. The justification behind choosing this thickness was it is thick enough to reliably tally absorbed dose, dose equivalent, and energy-dependent fluence in these regions, but not thick enough to substantially alter the radiation field.

Source

For each shielding configuration, February 1956 [13] and August 1972 [14] SPE boundary conditions were investigated. These historical SPEs represent hard and soft proton spectra, respectively, with differential energy spectra that monotonically decrease in the proton kinetic energy range from 10 keV to 2.5 GeV. The input boundary conditions were obtained directly from HZETRN-2015 [5-6]. The source geometry was modeled as a pencil beam incident on the center of the proximal slab to minimize edge effects resulting from particle leakage.

Transport Process

The absorbed dose, ICRP 60 dose equivalent [15], and energy-dependent fluence were tallied in the center water region for each shielding configuration. Radiation transport was simulated using PHITS 3.00 [8], a notable feature of which is an event generator that permits statistical sampling of charged particles from interactions involving neutrons with kinetic energies below 20 MeV. Additionally, PHITS is readily parallelizable, permitting the use of high-performance computing systems to reduce real simulation time.

For each combination of shielding material, thickness, and boundary conditions, seven importance weighting schemes were tested. These were labeled with indices ranging from 0 to 6, with 0 representing the PHITS default, which includes implicit scatter for all neutrons. Each index greater than 0 indicates the number of boundaries separating equal-thickness importance regions. A ratio of two was used to define the relative importance of neighboring regions, with the importance increasing in the front shield and decreasing in the back shield, as exhibited in Figure 1 for Importance Weighting Scheme Index 1. The water region was given the same importance as neighboring shield regions, equal to 2^i, where i represents importance weighting scheme index. These importance region definitions are based on the concept that the number of particle histories likely to contribute to the tally (i.e., particles moving toward the tally region in the proximal slab or reflected back towards the tally region in the distal slab) should be increased to improve computational efficiency. Similarly, computational resources spent tracking particle histories unlikely to contribute to the tally should be minimized.

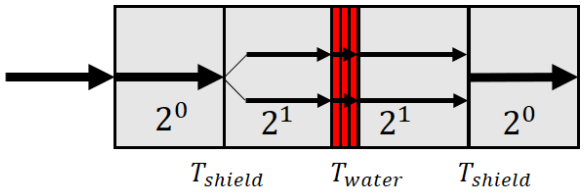

Fig. 1. Example importance weighting scheme.

Figure of Merit

The performance metric used to characterize efficiency of the is the figure of merit (FOM). If R is the relative error and T is the computation time of the MC method, then the FOM is given by:

$$FOM = \frac{1}{R^2 T} \quad (1)$$

The FOM is a stochastic quantity since both relative error and computation time vary with random seed. To ensure adequate sampling, simulations for each combination of SPE spectrum, shielding configuration, and importance weighting index were completed at least five times using the same number of source particles and the same node type. Using the Beocat cluster at Kansas State University, each simulation was completed on a single node consisting of two 10-Core Xeon E5-2630 v4 processors and 32 GB of RAM. Each job was submitted using the same script to nodes with the stated characteristics using 20-core shared memory (OpenMP) parallelization.

RESULTS

In this section, results for the February 1956 and August 1972 SPEs and various shielding configurations are presented for the seven importance weighting cases evaluated in this work. All FOMs presented are calculated using the absorbed dose tally, relevant for a detector with dose response characteristics equivalent to those of water. The average FOM and error bars representing one standard deviation are shown in all figures.

Generally, the results indicate that for thicker shields and softer SPE spectra, larger numbers of importance regions are warranted. Clearly, using Russian roulette and particle splitting in addition to implicit capture for neutrons can reduce the FOM. For 5 g cm^{-2} Al and HDPE shielding, no increase in FOM occurs beyond Importance Weighting Scheme Index 0, indicating a reduction in efficiency when the Russian roulette/particle splitting variance reduction method is implemented. An example case representing these thin shielding configurations is shown in Figure 2.

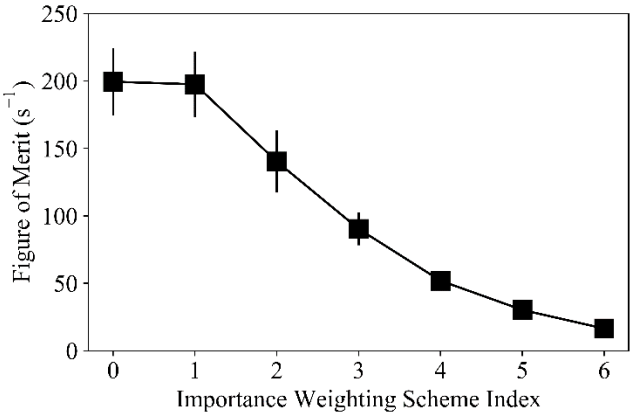

Fig. 2. FOM for Al with material thickness 5 g cm^{-2} for the August 1972 SPE.

Modest improvements in FOM are observed for shield thicknesses of 20 g cm^{-2} through use of Russian roulette and particle splitting. Results for the August 1972 SPE on Al shielding and the February 1956 SPE on HDPE shielding are shown in Figures 3 and 4, respectively. Better efficiency is realized as the Importance Weighting Scheme Index increases from 0 to a maximum at 2 or 3, followed by a substantial reduction in FOM as the index is increased

further. Maximum increases in FOM for these mid-range shielding configurations are limited to less than a factor of two, with the softer August 1972 SPE demonstrating larger increases in FOM than the harder February 1956 SPE for a given shielding configuration.

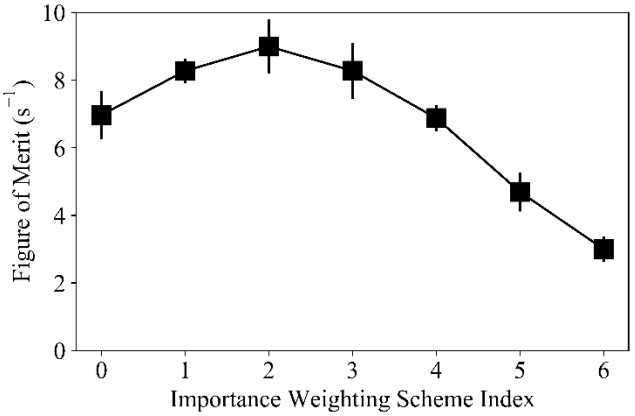

Fig. 3. FOM for Al with material thickness 20 g cm^{-2} for the August 1972 SPE.

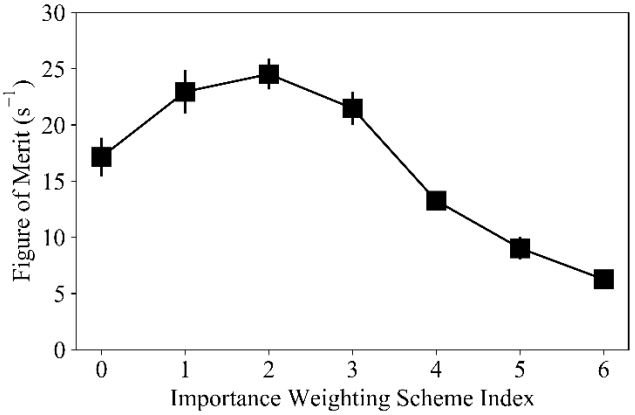

Fig. 4. FOM for HDPE with material thickness 20 g cm^{-2} for the February 1956 SPE.

The greatest potential for increase in computational efficiency occurs for the 100 g cm^{-2} shield thicknesses. For the February 1956 SPE, maximum FOM increases are again limited to less than a factor of two, and Importance Weighting Scheme Index 3, corresponding to four equal-thickness sublayers in the proximal and distal shields, exhibits the best computational efficiency. Results for the February 1956 SPE are shown in Figure 5 for Al and Figure 6 for HDPE. Maximum increases in FOM for the August 1972 SPE are around a factor of six, as exhibited for Al shielding in Figure 7. For HDPE (Figure 8), the maximum increase in FOM can exceed a factor of eight. Importance Weighting Scheme Indices 4-6 show the greatest potential for hastening simulations involving this softer SPE spectrum.

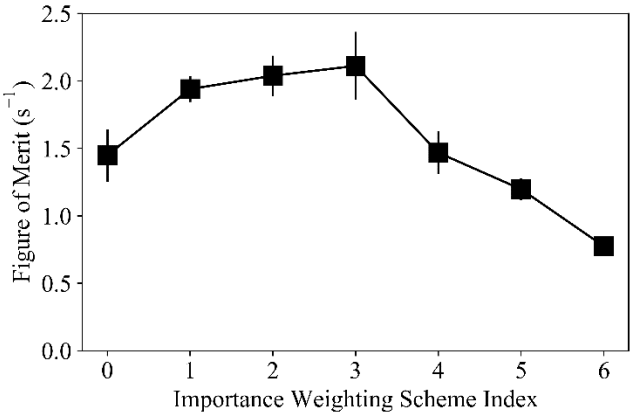

Fig. 5. FOM for Al with material thickness 100 g cm^{-2} for the February 1956 SPE.

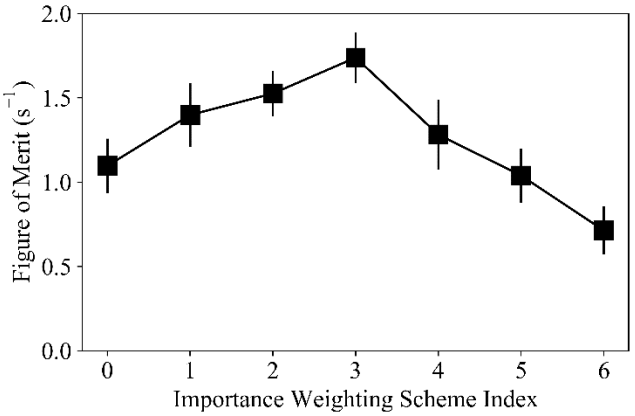

Fig. 6. FOM for HDPE with material thickness 100 g cm^{-2} for the February 1956 SPE.

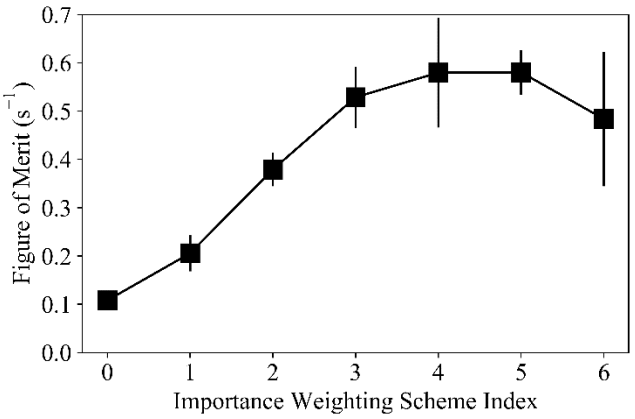

Fig. 7. FOM for Al with material thickness 100 g cm^{-2} for the August 1972 SPE.

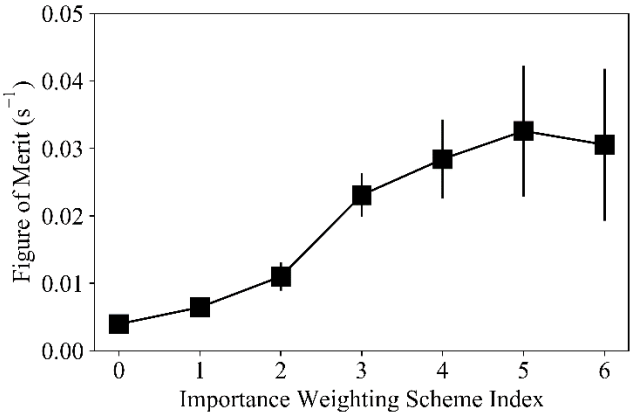

Fig. 8. FOM for HDPE with material thickness 100 g cm^{-2} for the August 1972 SPE.

This is the first known study to systematically evaluate the most efficient use of Russian roulette and particle splitting for space radiation transport for various combinations of shield material and thickness. It was found that this technique is ineffective for increasing computational efficiency for thin shielding, provides modest increases in FOM for intermediate shielding thicknesses, and results in the greatest improvement in FOM for thick shields and soft spectra. Beyond the maximum in FOM as a function of importance weighting scheme index, as more importance regions are used, the time required for tracking additional particles offsets reductions in tally variance, and a downward trend in the FOM is observed. While the simulation geometry and source were simplified in this study, these results provide valuable perspective on the use of this variance reduction method for more complicated problems.

In future work, similar approaches will be tested for GCR boundary conditions for solar minimum and solar maximum conditions, which present the greatest challenge in terms of simulation times due to the large number of secondary particles produced via projectile fragmentation. Further investigations will include the use of computational phantoms to represent human body self-shielding for calculation of organ dose equivalent using NASA quality factors [16], and investigation of non-uniform shield sublayer thicknesses.

REFERENCES

1. A. PAPAIOANNOU et al., "Solar flares, coronal mass ejections and solar energetic particle characteristics," *J. Space Weather Space Clim.*, **6**, *A42* (2016).
2. J. SIMPSON, "Elemental and isotopic composition of the galactic cosmic rays," *Ann. Rev. Nuc. Part. Sci.*, **33**, 323-381 (1983).
3. J. WILSON et al., "Issues in Deep Space Radiation Protection," *Acta Astronaut*. **49**, 289-312 (2001).
4. F. CUCINOTTA, M-H. KIM, L. REN, "Evaluating Shielding Effectiveness for Reducing Space Radiation Cancer Risks," Rad. Meas., **41**, 1173-1185 (2006).
5. NATIONAL RESEARCH COUNCIL, "*Pathways to Exploration: Rationales and Approaches for a U.S. Program of Human Space Exploration*," National Academic Press, Washington D.C, (2014).
6. T. SLABA, J. WILSON, F. BADAVI, B. REDDELL, A. BAHADORI, "Solar Proton Transport within an ICRU Sphere Surrounded by a Complex Shield: Ray-Trace Geometry," *NASA TP 2015-218994,* (2015).
7. T. SLABA, J. WILSON, F. BADAVI, B. REDDELL, A. BAHADORI, "Solar Proton Transport within an ICRU Sphere Surrounded by a Complex Shield: Combinatorial Geometry," *NASA TP 2015-218980,* (2015).
8. J. WILSON et al., "Advances in NASA radiation transport research: 3DHZETRN," *Life. Sci. Space. Res*. **2**, (2014).
9. T. SLABA, et al., "Coupled Neutron Transport for HZETRN," *J. Comput. Phys.,* **229**, (2010).
10. T. SATO et al., "Particle and Heavy Ion Transport Code System PHITS, Version 3.02," *J. Nucl. Sci. Technol*., (2018).
11. J. K. SHULTIS, R. E. FAW, "*Radiation Shielding*," Ch 11, pp. 420-425, American Nuclear Society, La Grange Park, (2000).
12. T. SLABA, et al., "Optimum Shielding Thickness for Galactic Cosmic Ray Environments," *Life. Sci. Space. Res.*, **12**, 1-15 (2017).
13. J. Wilson et al., "HZETRN: Description of a Free-Space ion and Nucleon Transport and Shielding Computer Program," *NASA TP-3495*, (1995).
14. J. KING, "Solar Proton Fluences for 1977-1983 Space Missions Space Missions," *Journal of Spacecrafts and Rockets.*, **11**, (1974).
15. ICRP, "1990 Recommendations of the International Commission on Radiological Protection. ICRP Publication 60," *Annals of the ICRP*, **21**, (1991).
16. F. CUCINOTTA, "Biophysics of NASA Radiation Quality Factors," *Radiat. Prot. Dosim.,* **166,** 282-289 (2015).